*British Journal of Nutrition* (2023), 129, 921–935 doi:10.1017/S0007114522001829


# Long non-coding RNA-EN_181 potentially contributes to the protective effects of N-acetylcysteine against non-alcoholic fatty liver disease in mice

Wenwen Yang[1,2]†, Rui Guo[1,4,5]†, Aiwen Pi[2], Qinchao Ding[1,5], Liuyi Hao[1,4,5], Qing Song[1,2], Lin Chen[1,4], Xiaobing Dou[2], Lixin Na[3] and Songtao Li[1,4,5]*

[1]*School of Public Health, Zhejiang Chinese Medical University, Hangzhou 310053, People's Republic of China*
[2]*School of Life Science, Zhejiang Chinese Medical University, Hangzhou, Zhejiang 310053, People's Republic of China*
[3]*Public Health College, Shanghai University of Medicine & Health Sciences, Shanghai 201318, People's Republic of China.*
[4]*Institute of Nutrition and Health, School of Public Health, Zhejiang Chinese Medical University, Hangzhou 310053, People's Republic of China*
[5]*Academy of Chinese Medical Science, Zhejiang Chinese Medical University, Hangzhou, Zhejiang 310053, People's Republic of China*

*(Submitted 26 November 2021 – Final revision received 8 May 2022 – Accepted 1 June 2022 – First published online 17 June 2022)*

## Abstract

N-acetylcysteine (NAC) possesses a strong capability to ameliorate high-fat diet (HFD)-induced non-alcoholic fatty liver disease (NAFLD) in mice, but the underlying mechanism is still unknown. Our study aimed to clarify the involvement of long non-coding RNA (lncRNA) in the beneficial effects of NAC on HFD-induced NAFLD. C57BL/6J mice were fed a normal-fat diet (10 % fat), a HFD (45 % fat) or a HFD plus NAC (2 g/l). After 14-week of intervention, NAC rescued the deleterious alterations induced by HFD, including the changes in body and liver weights, hepatic TAG, plasma alanine aminotransferase, plasma aspartate transaminase and liver histomorphology (haematoxylin and eosin and Oil red O staining). Through whole-transcriptome sequencing, 52 167 (50 758 known and 1409 novel) hepatic lncRNA were detected. Our cross-comparison data revealed the expression of 175 lncRNA was changed by HFD but reversed by NAC. Five of those lncRNA, lncRNA-NONMMUT148902·1 (NO_902·1), lncRNA-XR_001781798·1 (XR_798·1), lncRNA-NONMMUT141720·1 (NO_720·1), lncRNA-XR_869907·1 (XR_907·1), and lncRNA-ENSMUST00000132181 (EN_181), were selected based on an absolute $\log_2$ fold change value of greater than 4, *P*-value < 0·01 and *P*-adjusted value < 0·01. Further qRT-PCR analysis showed the levels of lncRNA-NO_902·1, lncRNA-XR_798·1, and lncRNA-EN_181 were decreased by HFD but restored by NAC, consistent with the RNA sequencing. Finally, we constructed a ceRNA network containing lncRNA-EN_181, 3 miRNA, and 13 mRNA, which was associated with the NAC-ameliorated NAFLD. Overall, lncRNA-EN_181 might be a potential target in NAC-ameliorated NAFLD. This finding enhanced our understanding of the biological mechanisms underlying the beneficial role of NAC.

**Key words:** **NAC: NAFLD: lncRNA: lncRNA-EN_181: RNA sequencing**

Non-alcoholic fatty liver disease (NAFLD) is considered the most common liver disease worldwide. It covers a wide range of pathological spectra, from simple steatosis to non-alcoholic steatohepatitis (NASH) and fibrosis, and eventually progresses to liver cirrhosis and hepatocellular carcinoma in some individuals[(1)]. As a multisystem disease[(2)], the prevalence of NAFLD usually parallels the prevalence of obesity[(3)], type 2 diabetes mellitus[(4)] and CVD[(5)]. Currently, there are no approved clinical treatments for NAFLD. It is estimated that NAFLD will probably emerge as the leading cause of end-stage liver disease in the coming decades.

C57BL/6J mice are commonly used to build high-fat diet (HFD)-induced NAFLD model[(6–8)]. Much progress has been made in the understanding of the potential mechanisms of NAFLD, among which oxidative stress plays a critical role in the initiation and development of various stages of NAFLD[(9)]. N-acetylcysteine (NAC) acts as a donor of cysteine, which leads to replenishment of glutathione, and thus serves clinically as an antioxidant[(10)]. Several studies have reported that NAC supplementation effectively improved HFD-induced hepatic steatosis and liver injury in experimental animal models of NAFLD[(11,12)]. NAC treatment also

**Abbreviations:** GO, Gene Ontology; HFD, high-fat diet; KEGG, Kyoto Encyclopaedia of Genes and Genomes Enrichment; lncRNA, long non-coding RNA; NAC, N-acetylcysteine; NAFLD, non-alcoholic fatty liver disease; NASH, non-alcoholic steatohepatitis.

* **Corresponding author:** Songtao Li, email lisongtao@zcmu.edu.cn

† These authors contributed equally to this work.

attenuated hepatic oxidative stress and improved liver fat deposition and necroinflammation in a male Sprague–Dawley rat model of HFD-induced NASH[13]. More strikingly, in a clinical trial, obvious improvements in liver steatosis and fibrosis were observed in NASH patients after treatment with NAC (1·2 g/d orally) for 12 months[14]. Several actions have been implicated in the beneficial effects of NAC, which include improving hepatic lipid metabolism[15], restoring the intestinal microecological balance[16] and alleviating liver inflammation[17]. However, the exact mechanisms underlying the protective effects of NAC against NAFLD are still largely unclear.

Long non-coding RNA (lncRNA), which contain more than 200 nucleotides, have emerged as new members in the regulation of multiple biological processes[18], such as chromatin structural modifications, transcription, miRNA activity and protein degradation. Recent evidence suggests that lncRNA are involved in multiple metabolic diseases, including NAFLD[19]. The liver lncRNA profiles can be altered in both patients and experimental model animals with NAFLD[20], among which a few lncRNA, including the lncRNA-MALAT1[21], lncRNA-NEAT1[22] and lncRNA RP11–484N16·1[23], have been reported to contribute to the pathological process of NAFLD. However, limited studies have addressed the involvement of lncRNA in NAC-mediated prevention of NAFLD.

In the present study, we confirmed that NAC supplementation effectively ameliorated HFD-induced hepatic steatosis and liver injury in NAFLD mice. Importantly, we observed that NAC intervention partially rescued HFD-stimulated dysregulation of the hepatic lncRNA profile, and we further identified lncRNA-EN_181 could be a potential target in the protective role of NAC via an lncRNA-miRNA-mRNA axis. This study provided novel insight helping us to understand the biological protective roles of NAC against hepatic metabolic diseases.

## Materials and methods

### Animal experiments

According to the recommendations of Care and Use of Laboratory Animals in China, our study was conducted and approved by the Animal Ethics Committee of Zhejiang Chinese Medical University (Approval No. ZSLL-2018–008). Twelve SPF male C57BL/6J mice (8 weeks old, body weight 22–25g) were purchased from Shanghai SLAC Laboratory Animal Co., Ltd (License No. SCXK(Hu)2017-0005). After a few days of adaptive feeding, mice were divided equally and randomly into three groups: the normal-fat diet (NFD, 10 % energy from fat) group, the HFD (45 % energy from fat) group and the HFD plus NAC (HFD + NAC, 2 g/L in the drinking water)[12] group. Mice were treated at a constant room temperature of 25°C on a 12/12-h light/dark cycle. Animals were provided with free access to water and food for 14 weeks; food/water intake was recorded daily and body weight was recorded weekly. Mice were euthanised by injection of barbital sodium (50 mg/kg body weight[24,25]) after 12 h of fasting, and blood and liver were harvested for further study.

### Biochemical assays

The activities of alanine aminotransferase and aspartate transaminase in plasma were measured according to the instructions of commercial kits (Nanjing Jiancheng Bioengineering Institute). The levels of TAG and total cholesterol in the liver were detected according to the instructions of total cholesterol and TAG kits (Applygen Technologies Inc.).

### Histological examination

Two small pieces of mouse liver tissue were immersed in 4 % paraformaldehyde for preparation of paraffin sections and frozen sections, and the sections were stained with haematoxylin and eosin and Oil red O (Nanjing Jiancheng Bioengineering Institute, Nanjing, China) for the evaluation of liver steatosis under a Nikon eclipse Ti-S fluorescence microscope (Nikon).

### Whole-transcriptome sequencing

Total RNA from the liver tissue was extracted using TRIzol[26–28] (Invitrogen), and genomic DNA was removed using rDNase I RNase-Free (TaKaRa). RNA quality was verified using an Agilent 2100 Bioanalyzer (Agilent Technologies) and the spectrophotometer (Thermo Fisher Scientific). High-quality RNA samples (OD 260/280 = 1·8~2·2, OD 260/230 ≥ 2·0, RIN ≥ 8, 28S/18S ≥ 1·0, > 10 μg) were used to construct a sequencing library. Five micrograms of RNA was used to construct the RNA sequencing transcriptome strand library using a TruSeqTM Stranded Total RNA Kit from Illumina. A Ribo-Zero Magnetic Kit was used to remove ribosomal RNA (rRNA) and then fragmented by fragmentation buffer firstly, and first-strand cDNA was synthesised with random hexamer primers. Then, the RNA template was removed and a replacement strand was synthesised, and AMPure XP beads were used to separate the ds cDNA, which was generated by incorporating dUTP in place of dTTP, from the second-strand reaction mix. Lastly, multiple indexing adapters were ligated to the ends of the ds cDNA. Libraries were selected for cDNA target fragments on 2 % Low Range Ultra Agarose followed by PCR amplified for fifteen PCR cycles. After quantified by TBS380, paired-end RNA-seq sequencing library was sequenced with the Illumina HiSeq xten//NovaSeq6000 (Illumina). In addition, 3 μg of total RNA was ligated with sequencing adapters with TruseqTM Small RNA Sample Prep Kit (Illumina). Subsequently, cDNA was synthesised by reverse transcription and amplified with twelve PCR cycles to produce libraries. After quantified by TBS380, deep sequencing was performed.

The raw paired-end reads were trimmed and quality controlled by SeqPrep (https://github.com/jstjohn/SeqPrep) and Sickle (https://github.com/najoshi/sickle) with default parameters. Then, clean reads were separately aligned to reference genome with orientation mode using HIASAT (https://ccb.jhu.edu/software/hisat2/index.shtml) software. The mapped reads for each sample were assembled by StringTie (https://ccb.jhu.edu/software/stringtie/index.shtml?t=example) via a reference-based approach. RSEM (http://deweylab.biostat.wisc.edu/rsem/) was used to quantify gene abundances.

Transcripts that overlapped with known protein-coding genes on the same strand, transcripts with fragment count ≤ 3, transcripts shorter than 200 nt, the open reading frame longer than 300 nt and an exon number of less than 2 were discarded. Then, we used the Coding Potential Calculator[29] and Coding-Non-Coding index[30] to filter transcripts with coding potential. The remained transcripts were considered reliably expressed lncRNA.

### Quantitative real-time PCR

Total RNA was extracted from liver tissue with TRIzol, and a cDNA Synthesis Kit (Vazyme) was used to convert RNA into cDNA. cDNA, $ddH_2O$, SYBR qPCR Master Mix (Vazyme) and primers were mixed together for qRT-PCR in a CFX-96Touch thermal cycler (Hercules) with the following programmes: 95°C for 30 s for denaturation with Hot-Start DNA Polymerase; 40 cycles at 95°C for 15 s and 60°C for 1 min for PCR amplification and 95°C for 15 s, 60°C for 1 min and 95°C for 15 s for melt curve analysis. The $2^{-\Delta\Delta Ct}$ method was used to calculate the relative expression of candidate lncRNA. The primer sequences specific for the candidate lncRNA are listed in Supplementary Table 1.

### Gene Ontology and Kyoto Encyclopaedia of Genes and Genomes Enrichment Analyses

GO functional enrichment analysis was performed to calculate the number of all mRNA coexpressed with the 175 known lncRNA and map the mRNA to each term in the GO database. GO has three categories that describe the molecular function of a gene, the cellular component where its product performs its function and the biological process in which its product participates. First, the top fifty GO terms were selected based on the number of mRNA associated with the GO terms. Then, according to the most significantly enriched GO terms with the highest rich factor, fifteen GO terms were selected. In addition, the fifteen most significantly enriched KEGG pathways were identified using the same method.

### Long non-coding RNA-associated ceRNA network construction

miRanda and RNAhybrid were used to predict miRNA-lncRNA and miRNA–mRNA interactions. To increase the reliability of our results, only interactions found in both databases were converted into lncRNA-miRNA–mRNA interactions, according to the ceRNA hypothesis (ceRNA include lncRNA and mRNA competing for an miRNA). Moreover, we removed some RNA that did not meet the criterion of negative regulation between lncRNA and miRNA or between miRNA and mRNA. Finally, Cytoscape software (v3.8.2, http://www.cytoscape.org/) was used to construct the lncRNA-associated ceRNA network.

### Statistical analysis

Statistical analysis was performed with SPSS 25.0 software using one-way ANOVA (comparisons among multiple groups) followed by Fisher's least significant difference post hoc test. All data were expressed as the means ± standard deviation (SD) with at least three replicates in each experiment. Statistical significance was assumed at $P < 0{\cdot}05$.

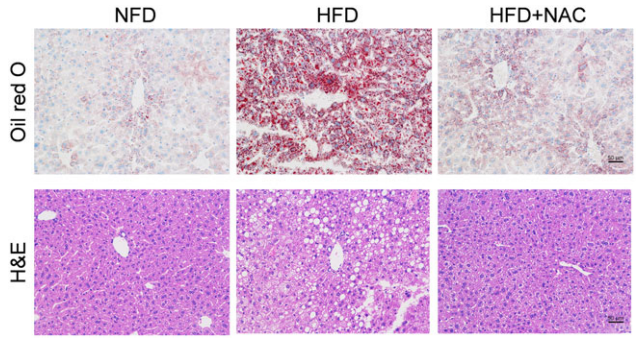


**Fig. 1.** NAC ameliorates HFD-induced liver dysfunction. Histological analysis was performed by Oil red O and H&E staining of liver samples (200x). NFD, normal fat diet; HFD, high-fat diet; NAC, N-acetylcysteine. *n* 4 mice per group.

## Results

### N-acetylcysteine ameliorates high-fat diet-induced liver dysfunction

The obesity-associated NAFLD mouse model was successfully established after 14 weeks of HFD feeding, as evidenced by haematoxylin and eosin and Oil red O staining (Fig. 1) and body weight, liver weight, hepatic TAG content, plasma alanine aminotransferase level and aspartate transaminase level measurement (Table 1). Notably, the HFD-induced detrimental alterations mentioned above were largely rescued by 14 weeks of NAC treatment (Fig. 1 and Table 1).

### The profiles and differential expression of long non-coding RNA in high-fat diet and N-acetylcysteine-treated mice

A total of 52 167 lncRNA, namely 50 758 known and 1409 novel lncRNA, were detected in liver samples by whole-transcriptome sequencing. The volcano plots show the variations in known lncRNA between the NFD and HFD groups as well as the HFD + NAC and HFD groups (Fig. 2(a) and (b)). A total of 175 lncRNA with significant differences were filtered out based on FC ≥ 2 or ≤ 0·5[24,25], which meant that the HFD-induced alterations in lncRNA expression were significantly reversed by NAC treatment, as shown in the Venn diagrams (Fig. 2(c) and (d)) and Table 2. Among those lncRNA, 123 were down-regulated in the HFD group compared with the NFD group, while those lncRNA were up-regulated by NAC treatment compared with their expression in the HFD group (Fig. 2(c)); the other fifty-two lncRNA were up-regulated in the HFD group compared with the NFD group, while NAC treatment reduced their expression (Fig. 2(d)). The differential lncRNA expression profiles in NFD-, HFD- and HFD + NAC-treated mouse livers were distinguishable in a heatmap generated by hierarchical clustering (Fig. 2(e)).

The relevant raw data can be viewed according to GSE188128 provided by GEO.

**Table 1.** Biochemical parameters in mice

| | NFD | | HFD | | HFD + NAC | |
|---|---|---|---|---|---|---|
| | Mean | SD | Mean | SD | Mean | SD |
| Body weight (g) | 27·85 | 0·54 | 39·55 | 0·52* | 34·26 | 1·64*,† |
| Liver weight (g) | 1·16 | 0·07 | 1·43 | 0·12* | 1·16 | 0·07† |
| Liver TC (μM/g liver weight) | 5·64 | 0·25 | 5·93 | 0·46 | 6·33 | 0·33 |
| Liver TG (μM/g liver weight) | 37·62 | 2·88 | 55·30 | 1·49* | 44·77 | 1·98*,† |
| Plasma ALT (μg/l) | 13·03 | 2·12 | 28·32 | 7·19* | 15·46 | 2·69† |
| Plasma AST (μg/l) | 26·84 | 6·05 | 38·83 | 2·14* | 25·16 | 4·57† |

NFD, normal fat diet; HFD, high-fat diet; NAC, N-acetylcysteine. TC, total cholesterol; ALT, alanine aminotransferase; AST, aspartate transaminase. *n* 4 per group.
* $P < 0.05$ *v.* NFD.
† $P < 0.05$ *v.* HFD.

### *Gene Ontology and Kyoto Encyclopedia of Genes and Genomes Enrichment analyses*

As shown in Fig. 3(a), GO analysis of the host genes of the 175 lncRNA was performed based on the biological process, cellular component and molecular function categories. The biological process analysis showed that those lncRNA were enriched in the regulation of response to external stimulus and single-organism metabolic process. The cellular component analysis indicated that those lncRNA were enriched in the mitochondrial inner membrane and organelle inner membrane. The molecular function analysis showed that oxidoreductase activity and carbohydrate kinase activity were the top two enriched terms. Furthermore, the KEGG analysis of the host genes predicted fifteen significantly enriched pathways (Fig. 3(b)), among which the notably enriched pathways were peroxisome and NOD-like receptor signalling pathway.

### *Validation of candidate long non-coding RNA*

Based on the more stringent parameter selection criteria of an absolute $\log_2$ (FC) ≥ 4, a *P* value ≤ 0·01 and a *P*-adjust ≤ 0·01, five lncRNA among those 175 lncRNA were selected for further analysis. The characteristics of these five lncRNA are shown in italics in Table 2. We subsequently tested the expression of these five lncRNA using qRT-PCR, and the results indicated that the expression levels of lncRNA-NO_902·1, lncRNA-XR_798·1 and lncRNA-EN_181 were consistent with the RNA sequencing results (Fig. 4). Our data indicated that the expression of lncRNA-NO_902·1, lncRNA-XR_798·1 and lncRNA-EN_181 was dramatically decreased by HFD feeding compared with NFD feeding, while NAC supplementation significantly reversed these alterations (Fig. 4).

### *Construction of the lncRNA-EN_181-associated ceRNA network*

According to the miRanda and RNAhybrid databases, no miRNA were predicted to interact with lncRNA-NO_902·1 and lncRNA-XR_798·1. Interacting miRNA were predicted for only lncRNA-EN_181 and included miR-6937–5p, miR-378d and miR-1955–5p after taking the intersection of the predictions from the two databases. Subsequently, mRNA were retrieved based on both the above-mentioned miRNA predicted using the miRanda and RNAhybrid databases and the results of RNA sequencing (mRNA with the same expression trends as lncRNA-EN_181 were selected as candidates). After intersection of these data sets, thirteen mRNA (Table 3) – *St5*, *Slc5a6*, *Fzr1*, *Arhgef3*, *Cd81*, *Unc13d*, *Arid1b*, *Slc13a2*, *Dgcr2*, *Ahsg*, *Zfp639*, *Abcb8* and *Pard3* – were predicted as target genes of lncRNA-EN_181 by mediating predicted miRNA. The lncRNA-EN_181-associated ceRNA network was successfully constructed in our study using Cytoscape software (Fig. 5).

### *The expressions of microRNA and mRNA corresponding to lncRNA-EN_181 by qRT-PCR*

We further validated the constructed ceRNA network by measuring the predicted miRNA and their target mRNA. Our data indicated that the expressions of miR-378d, miR-6937–5p and miR-1955–5p were all up-regulated by HFD compared with NFD, while NAC supplementation significantly reversed these alterations (Fig. 6(a)). Furthermore, the expressions of *Zfp639*, *Ahsg*, *Dgcr2*, *Unc13d*, *Fzr1* and *Slc5a6* were down-regulated by HFD compared with NFD, while NAC supplementation significantly rescued their alterations. However, the expressions of *Pard3*, *Arhgef3*, *Cd81*, *St5* and *Abcb8* were not statistically different under HFD and NAC interventions (Fig. 6(b)).

## Discussion

In the current study, we confirmed that lncRNA-EN_181 was obviously down-regulated in the livers of mice fed a HFD and that its expression was restored by NAC treatment. In addition, based on bioinformatics analysis, we predicted an lncRNA-EN_181-related ceRNA network containing three miRNA and thirteen mRNA that might be involved in both the pathological process of NAFLD and the beneficial effect of NAC.

NAFLD has become the most prevalent chronic liver disease worldwide. Although the understanding of the pathogenesis of NAFLD has improved, the exact underlying mechanism(s) are largely unclear, which limits the prevention and treatment of this disease. In the pathological process of NAFLD, many biomolecules, including DNAs, RNA, and proteins, are affected by metabolic reprogramming. Among those biomolecules, it is difficult to identify which changed biomolecules can be used as potential targets for the prevention and treatment of this disease. Therefore, we proposed exploring potential targets by searching for biomolecules whose dysregulation may be ameliorated by effective drugs. In this study, NAC, which has been reported to alleviate NAFLD in both experimental animals[31] and human patients[32], was employed to ameliorate HFD-induced obese-associated NAFLD in mice. The dosage of NAC used in animal studies ranged from 20 g/kg/d[33] to 1000 mg/kg/d[34]. NAC was also supplied in the drinking water at a concentration of 2 g/l in our study, according to a previous study[12]. According to the amount of drinking water, the NAC intake of each mouse at this dose is about 500 mg /kg body weight, which is in the middle dose of the existing literature. The dosage of NAC used in human beings ranged from 600 mg/d[35] to 9 g/d[36]. By searching the literature, we found that there were reports of 9 g/d dose intervention for 24 weeks in the population study[37], and no serious adverse reactions caused by NAC were found in this trial. Some studies also

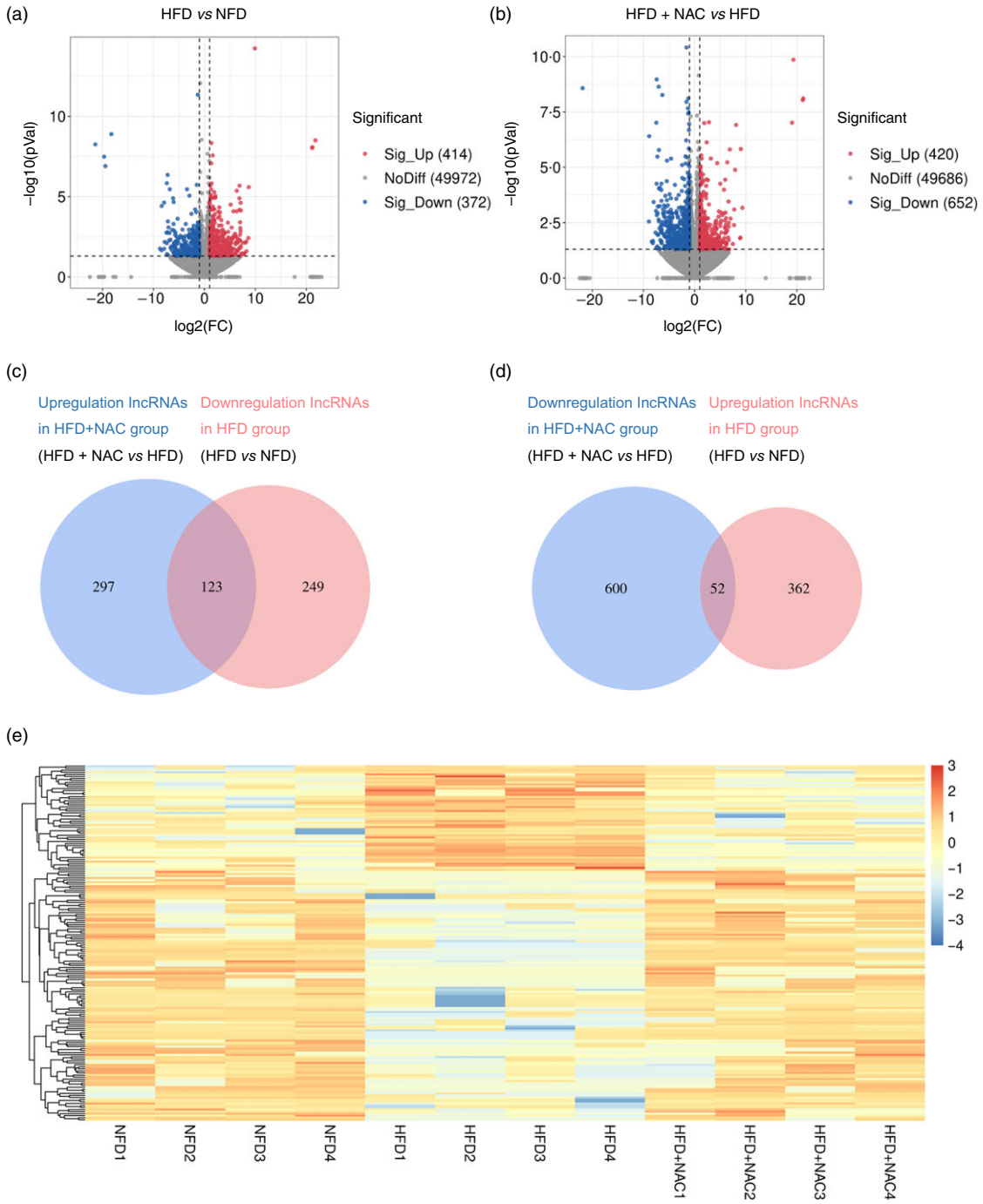


**Fig. 2.** The profiles and differential expression of lncRNA in HFD- and NAC-treated mice. (a) and (b) Volcano plot showing the differentially expressed lncRNA. The red dots represent the up-regulated lncRNA, and the blue dots represent the down-regulated lncRNA. The vertical lines correspond to 2-fold up-regulation and down-regulation. The horizontal line indicates a *P* value = 0·05. (c) and (d) Venn diagrams showing overlapping lncRNA between differentially expressed lncRNA in the HFD *v.* the NFD group and the HFD + NAC *v.* the HFD group. (e) Heatmap of the hierarchical clustering analysis of lncRNA. The scale bar indicates the level of lncRNA expression. Red, higher level of expression; blue, lower level of expression.

suggested that better results may be achievable in a longer NAC follow-up[11]. In addition, several studies have also revealed the beneficial role of NAC on HFD-increased blood lipids and glucose[16,27,38]. In line with the existing evidence, we observed that NAC supplementation significantly reversed HFD-induced hepatic steatosis and liver injury in NAFLD mice.

Emerging evidence has shown that non-coding RNA, such as microRNA, lncRNA and circRNA, are implicated in the pathogenesis of NAFLD[39,40]. To date, limited studies have addressed whether and how lncRNA contribute to the protective role of NAC. In this study, 52 167 lncRNA, namely 50 758 known and 1409 novel lncRNA, were detected by whole-transcriptome

**Table 2.** The characteristics of 175 lncRNA

| lncRNA | Full name | Genomic location | Characteristic | HFD/NFD | | | HFD + NAC/HFD | | |
|---|---|---|---|---|---|---|---|---|---|
| | | | | $Log_2FC$ | *P* | Regulation | $Log_2FC$ | *P* | Regulation |
| EN_275 | ENSMUST00000132275 | Chr8:123102652–123104464 | sense_exon_overlap | −6·1658 | ≤ 0·0001 | down | 6·3875 | ≤ 0·0001 | up |
| XR_376·2 | XR_388376·2 | Chr11:78188524–78192193 | sense_exon_overlap | −5·2753 | 0·0002 | down | 4·2766 | 0·0035 | up |
| EN_187 | ENSMUST00000159187 | Chr12:81581677–81595008 | sense_exon_overlap | −5·0734 | 0·0075 | down | 4·7118 | 0·0134 | up |
| EN_064 | ENSMUST00000171064 | Chr16:38585492–38586639 | sense_exon_overlap | −1·1953 | 0·0390 | down | 1·2627 | 0·0293 | up |
| EN_667 | ENSMUST00000152667 | Chr16:4 769 308–4 790 266 | sense_exon_overlap | −3·3850 | 0·0473 | down | 5·3257 | 0·0014 | up |
| EN_752 | ENSMUST00000150752 | Chr1:150430423–150440312 | sense_exon_overlap | −1·7028 | 0·0092 | down | 1·8983 | 0·0037 | up |
| EN_527 | ENSMUST00000214527 | Chr10:93474234–93483001 | sense_exon_overlap | −1·6784 | 0·0051 | down | 1·4758 | 0·0148 | up |
| EN_944 | ENSMUST00000147944 | Chr2:174469171–174472891 | sense_exon_overlap | −4·0020 | 0·0043 | down | 4·2106 | 0·0025 | up |
| XR_538·3 | XR_374538·3 | Chr2:163602280–163619013 | sense_exon_overlap | −2·5035 | 0·0478 | down | 2·6103 | 0·0391 | up |
| XR_774·1 | XR_001783774·1 | Chr3:94994409–95015413 | sense_exon_overlap | −4·4602 | 0·0102 | down | 3·9113 | 0·0244 | up |
| XR_057·3 | XR_380057·3 | Chr10:39732068–39854717 | sense_exon_overlap | −2·8270 | 0·0204 | down | 2·4357 | 0·0461 | up |
| EN_178 | ENSMUST00000129178 | Chr10:86690208–86701968 | sense_exon_overlap | −1·3008 | 0·0047 | down | 1·1313 | 0·0140 | up |
| NO_735·2 | NONMMUT007735·2 | Chr10:121780993–121781989 | sense_exon_overlap | −3·6044 | 0·0160 | down | 3·1919 | 0·0344 | up |
| EN_386 | ENSMUST00000154386 | Chr11:59184155–59184854 | sense_exon_overlap | −2·2227 | 0·0207 | down | 1·9956 | 0·0399 | up |
| EN_632 | ENSMUST00000222632 | Chr12:98784835–98786848 | sense_exon_overlap | −1·8109 | 0·0118 | down | 1·5830 | 0·0288 | up |
| EN_052 | ENSMUST00000124052 | Chr13:21179957–21181707 | sense_exon_overlap | −1·2153 | 0·0178 | down | 1·2752 | 0·0130 | up |
| XR_730·3 | XR_382730·3 | Chr13:92487100–92530922 | sense_exon_overlap | −7·2626 | 0·0017 | down | 7·7351 | 0·0008 | up |
| XR_130·1 | XR_001781130·1 | Chr14:99099772–99254494 | sense_exon_overlap | −6·0328 | 0·0077 | down | 5·0665 | 0·0259 | up |
| XR_082·1 | XR_001781082·1 | Chr14:120275661–120431698 | sense_exon_overlap | −8·4308 | 0·0219 | down | 8·9527 | 0·01496 | up |
| XR_520·1 | XR_001781520·1 | Chr15:12117792–12185449 | sense_exon_overlap | −1·1148 | 0·0101 | down | 1·1400 | 0·0086 | up |
| EN_097 | ENSMUST00000160097 | Chr15:76351352–76352067 | sense_exon_overlap | −3·6738 | 0·0352 | down | 5·0249 | 0·0032 | up |
| XR_828·1 | XR_001781828·1 | Chr16:55973272–56008913 | sense_exon_overlap | −5·6357 | 0·0488 | down | 6·1702 | 0·0308 | up |
| EN_507 | ENSMUST00000148507 | Chr16:20540752–20541871 | sense_exon_overlap | −3·3333 | 0·0225 | down | 3·9304 | 0·0067 | up |
| NR_488·1 | NR_027488·1 | Chr16:22009483–22049269 | sense_exon_overlap | −1·2298 | 0·0166 | down | 1·0524 | 0·0406 | up |
| *XR_798·1* | *XR_001781798·1* | *Chr16:91647842–91679725* | *sense_exon_overlap* | *−21·4375* | *≤ 0·0001* | *down* | *21·1438* | *≤ 0·0001* | *up* |
| XR_593·1 | XR_001784593·1 | Chr5:137288284–137294461 | sense_exon_overlap | −4·5949 | 0·0166 | down | 4·2187 | 0·0289 | up |
| EN_088 | ENSMUST00000176088 | Chr18:60828066–60829027 | sense_exon_overlap | −2·1366 | 0·0067 | down | 1·8256 | 0·0225 | up |
| EN_987 | ENSMUST00000128987 | Chr19:12695803–12714831 | sense_exon_overlap | −1·1266 | 0·0287 | down | 1·3600 | 0·0083 | up |
| EN_623 | ENSMUST00000237623 | Chr19:18758624–18824425 | sense_exon_overlap | −3·9553 | 0·0395 | down | 4·1993 | 0·0284 | up |
| XR_455·3 | XR_386455·3 | Chr19:55741786–55933661 | sense_exon_overlap | −5·2104 | 0·0045 | down | 7·9139 | ≤ 0·0001 | up |
| EN_090 | ENSMUST00000163090 | Chr19:39802608–39807430 | sense_exon_overlap | −1·7421 | 0·0030 | down | 1·6500 | 0·0050 | up |
| EN_046 | ENSMUST00000176046 | Chr19:46284562–46285980 | sense_exon_overlap | −3·7333 | 0·0028 | down | 4·9998 | ≤ 0·0001 | up |
| XR_762·1 | XR_870762·1 | Chr9:59617288–59650290 | sense_exon_overlap | −5·4617 | 0·0032 | down | 6·0221 | 0·0011 | up |
| NO_588·2 | NONMMUT035588·2 | Chr2:10254092–10256526 | sense_intron_overlap | −1·8195 | ≤ 0·0001 | down | 1·0864 | 0·0193 | up |
| EN_160 | ENSMUST00000195160 | Chr1:36553223–36554230 | sense_exon_overlap | −4·8465 | 0·0038 | down | 4·0522 | 0·0169 | up |
| EN_603 | ENSMUST00000134603 | Chr1:87756092–87767983 | sense_exon_overlap | −3·2880 | 0·0417 | down | 3·3565 | 0·0376 | up |
| EN_467 | ENSMUST00000185467 | Chr1:119595441–119599240 | sense_exon_overlap | −3·3230 | 0·0195 | down | 3·3516 | 0·0186 | up |
| EN_201 | ENSMUST00000125201 | Chr2:4 999 020–5 005 099 | sense_exon_overlap | −1·2888 | 0·0417 | down | 2·5954 | ≤ 0·0001 | up |
| EN_290 | ENSMUST00000136290 | Chr2:23517802–23537500 | sense_exon_overlap | −4·3100 | 0·0192 | down | 3·9764 | 0·0319 | up |
| EN_595 | ENSMUST00000155595 | Chr2:34773665–34774333 | sense_exon_overlap | −1·7984 | 0·0037 | down | 1·5953 | 0·0100 | up |
| EN_466 | ENSMUST00000145466 | Chr2:34772580–34774192 | sense_exon_overlap | −1·9100 | 0·0107 | down | 2·0061 | 0·0074 | up |
| EN_333 | ENSMUST00000129333 | Chr2:34774846–34775615 | sense_exon_overlap | −2·3616 | 0·0011 | down | 2·0387 | 0·0050 | up |
| EN_450 | ENSMUST00000130450 | Chr2:121424629–121432136 | sense_exon_overlap | −1·4547 | 0·0068 | down | 1·0983 | 0·0417 | up |
| XR_729·1 | XR_001783729·1 | Chr3:54692759–54728763 | sense_exon_overlap | −1·6267 | 0·0013 | down | 1·4770 | 0·0035 | up |
| EN_519 | ENSMUST00000159519 | Chr3:75517275–75521030 | sense_exon_overlap | −3·1290 | 0·0027 | down | 2·6607 | 0·0123 | up |
| EN_232 | ENSMUST00000127232 | Chr3:108075363–108076432 | sense_exon_overlap | −5·0379 | 0·0310 | down | 4·6961 | 0·04506 | up |
| XR_172·1 | XR_001784172·1 | Chr4:43002336–43010567 | sense_exon_overlap | −5·5043 | 0·0188 | down | 6·1605 | 0·0084 | up |
| EN_895 | ENSMUST00000135895 | Chr4:43578982–43579622 | sense_exon_overlap | −3·5808 | 0·0165 | down | 3·0979 | 0·0411 | up |
| EN_755 | ENSMUST00000150755 | Chr4:109304464–109305927 | sense_exon_overlap | −3·4733 | 0·0116 | down | 3·9212 | 0·0042 | up |

**Table 2.** (*Continued*)

| lncRNA | Full name | Genomic location | Characteristic | HFD/NFD | | | HFD + NAC/HFD | | |
|---|---|---|---|---|---|---|---|---|---|
| | | | | $Log_2FC$ | *P* | Regulation | $Log_2FC$ | *P* | Regulation |
| EN_376 | ENSMUST00000133376 | Chr5:37319190–37336878 | sense_exon_overlap | −4·1362 | 0·0108 | down | 3·6822 | 0·0252 | up |
| EN_877 | ENSMUST00000122877 | Chr5:115945296–115998498 | sense_exon_overlap | −4·5118 | 0·0116 | down | 3·7123 | 0·0398 | up |
| EN_555 | ENSMUST00000197555 | Chr5:144009221–144014877 | sense_exon_overlap | −1·3806 | 0·0097 | down | 1·1487 | 0·0328 | up |
| EN_949 | ENSMUST00000203949 | Chr6:145864662–145865352 | sense_intron_overlap | −3·0453 | 0·0012 | down | 2·3190 | 0·0151 | up |
| XR_030·2 | XR_878030·2 | ChrX:8 193 845–8 206 546 | sense_exon_overlap | −5·0866 | 0·0303 | down | 5·0254 | 0·0325 | up |
| NO_649·2 | NONMMUT073649·2 | ChrX:107782761–107784831 | sense_exon_overlap | −1·9447 | 0·0179 | down | 1·7985 | 0·0292 | up |
| EN_249 | ENSMUST00000210249 | Chr8:13884793–13887215 | sense_exon_overlap | −3·0114 | 0·0037 | down | 2·2780 | 0·0322 | up |
| NR_367·1 | NR_028367·1 | Chr8:107056876–107060931 | sense_exon_overlap | −4·3088 | 0·0140 | down | 4·1868 | 0·0170 | up |
| EN_112 | ENSMUST00000160112 | Chr9:44379583–44386070 | sense_exon_overlap | −1·6672 | 0·0033 | down | 1·2470 | 0·0283 | up |
| EN_737 | ENSMUST00000184737 | Chr9:72662437–72672148 | sense_exon_overlap | −2·1298 | 0·0007 | down | 1·3042 | 0·0430 | up |
| EN_750 | ENSMUST00000228750 | Chr17:24587618–24591416 | sense_exon_overlap | −1·9693 | 0·0047 | down | 1·6304 | 0·0204 | up |
| NO_053·2 | NONMMUT040053·2 | Chr2:134594508–134596832 | sense_exon_overlap | −5·9686 | 0·0089 | down | 7·0147 | 0·0021 | up |
| XR_043·1 | XR_001783043·1 | Chr2:39066216–39190734 | sense_exon_overlap | −3·8741 | 0·0112 | down | 4·2282 | 0·0056 | up |
| NO_857·2 | NONMMUT036857·2 | Chr2:35100852–35101559 | intergenic | −1·2005 | 0·0280 | down | 1·6555 | 0·0023 | up |
| EN_712 | ENSMUST00000212712 | Chr8:95734312–95736729 | sense_exon_overlap | −1·6706 | 0·0187 | down | 1·9332 | 0·0064 | up |
| EN_786 | ENSMUST00000227786 | Chr17:15044394–15048728 | sense_exon_overlap | −3·0484 | 0·0024 | down | 4·4203 | ≤ 0·0001 | up |
| EN_737 | ENSMUST00000234737 | Chr18:14655090–14670786 | sense_exon_overlap | −1·9631 | 0·0017 | down | 1·7784 | 0·0050 | up |
| EN_916 | ENSMUST00000123916 | Chr3:36863120–36943396 | sense_exon_overlap | −5·9838 | 0·0013 | down | 6·6353 | 0·0003 | up |
| XR_545·1 | XR_001781545·1 | Chr15:55015128–55072193 | sense_exon_overlap | −5·4845 | 0·0096 | down | 5·9229 | 0·0051 | up |
| EN_250 | ENSMUST00000173250 | Chr1:36146156–36150524 | sense_exon_overlap | −2·1566 | 0·0020 | down | 2·1456 | 0·0022 | up |
| EN_835 | ENSMUST00000140835 | Chr6:125009744–125032787 | sense_exon_overlap | −6·6690 | 0·0048 | down | 6·6832 | 0·0047 | up |
| XR_168·1 | XR_001785168·1 | Chr6:35177715–35247557 | sense_exon_overlap | −7·4098 | 0·0079 | down | 6·1959 | 0·0267 | up |
| EN_342 | ENSMUST00000202342 | Chr5:54115856–54118587 | sense_exon_overlap | −1·7419 | 0·0295 | down | 2·1721 | 0·0063 | up |
| EN_093 | ENSMUST00000133093 | ChrX:8 154 482–8 175 958 | sense_exon_overlap | −1·7012 | 0·0121 | down | 1·5959 | 0·0191 | up |
| NO_216·2 | NONMMUT005216·2 | Chr10:33950779–33951212 | sense_intron_overlap | −1·1680 | 0·0480 | down | 1·4322 | 0·0144 | up |
| EN_730 | ENSMUST00000236730 | Chr19:45921272–45936429 | sense_exon_overlap | −2·5363 | 0·0066 | down | 2·2447 | 0·0176 | up |
| EN_631 | ENSMUST00000235631 | Chr19:27409729–27421483 | sense_exon_overlap | −1·0770 | 0·0092 | down | 1·0691 | 0·0099 | up |
| EN_125 | ENSMUST00000161125 | Chr1:52845043–52885337 | sense_exon_overlap | −2·3186 | 0·0056 | down | 1·7717 | 0·0369 | up |
| EN_568 | ENSMUST00000196568 | Chr3:90015017–90052331 | sense_exon_overlap | −5·7208 | 0·0453 | down | 6·6694 | 0·0194 | up |
| XR_163·3 | XR_387163·3 | Chr1:152954970–153119266 | sense_exon_overlap | −4·0838 | 0·0057 | down | 3·8512 | 0·0094 | up |
| XR_516·3 | XR_386516·3 | Chr19:10634212–10656703 | sense_exon_overlap | −2·9207 | 0·0020 | down | 2·4394 | 0·0103 | up |
| EN_140 | ENSMUST00000137140 | Chr5:115124961–115127513 | sense_exon_overlap | −5·4616 | 0·0060 | down | 6·1355 | 0·0020 | up |
| EN_588 | ENSMUST00000125588 | Chr5:124451170–124460837 | sense_exon_overlap | −6·3767 | 0·0012 | down | 5·9419 | 0·0025 | up |
| XR_042·3 | XR_384042·3 | Chr15:58904794–58933756 | sense_exon_overlap | −6·0857 | 0·0005 | down | 5·0179 | 0·0045 | up |
| *EN_181* | *ENSMUST00000132181* | *Chr7:66710145–66717254* | *sense_exon_overlap* | *−7·2270* | *≤ 0·0001* | *down* | *6·8844* | *≤ 0·0001* | *up* |
| EN_267 | ENSMUST00000196267 | Chr5:139363650–139460511 | sense_exon_overlap | −3·7902 | 0·0183 | down | 3·7009 | 0·0216 | up |
| XR_752·2 | XR_868752·2 | Chr5:151416418–151423964 | antisense | −5·8058 | 0·0145 | down | 6·3960 | 0·0070 | up |
| EN_955 | ENSMUST00000153955 | Chr5:105519472–105544640 | sense_exon_overlap | −4·3152 | 0·0011 | down | 3·4941 | 0·0098 | up |
| XR_858·1 | XR_001779858·1 | Chr11:116837431–116843360 | sense_exon_overlap | −7·1909 | 0·0004 | down | 4·3026 | 0·0353 | up |
| EN_265 | ENSMUST00000165265 | Chr7:31070536–31076655 | sense_exon_overlap | −3·4687 | 0·0194 | down | 4·7307 | 0·0010 | up |
| EN_893 | ENSMUST00000234893 | Chr17:33646235–33648979 | sense_exon_overlap | −2·9142 | 0·0266 | down | 3·5819 | 0·0059 | up |
| XR_623·1 | XR_001784623·1 | Chr5:134237833–134314760 | sense_exon_overlap | −1·7698 | 0·0162 | down | 1·8754 | 0·0108 | up |
| XR_678·1 | XR_001784678·1 | Chr5:108571514–108629777 | sense_exon_overlap | −5·8298 | 0·0110 | down | 5·9624 | 0·0093 | up |
| XR_888·2 | XR_868888·2 | Chr6:71880637–71908772 | sense_exon_overlap | −6·8910 | 0·0019 | down | 4·5609 | 0·0417 | up |
| XR_165·1 | XR_001785165·1 | Chr6:71880637–71908772 | sense_exon_overlap | −18·2887 | ≤ 0·0001 | down | 19·3154 | ≤ 0·0001 | up |
| NO_366·1 | NONMMUT153366·1 | Chr9:74847982–74861734 | intergenic | −1·9144 | 0·0086 | down | 1·9018 | 0·0090 | up |
| EN_506 | ENSMUST00000189506 | Chr1:54554602–54557627 | sense_intron_overlap | −1·0315 | 0·0304 | down | 1·1217 | 0·0186 | up |
| EN_329 | ENSMUST00000150329 | Chr11:16815430–16830702 | antisense | −2·5824 | 0·0416 | down | 3·1550 | 0·0124 | up |
| NO_069·1 | NONMMUT148069·1 | Chr4:62722110–62725388 | intergenic | −4·0720 | 0·0342 | down | 4·3067 | 0·0248 | up |

**Table 2.** (*Continued*)

| lncRNA | Full name | Genomic location | Characteristic | HFD/NFD | | | HFD + NAC/HFD | | |
|---|---|---|---|---|---|---|---|---|---|
| | | | | $Log_2FC$ | *P* | Regulation | $Log_2FC$ | *P* | Regulation |
| EN_647 | ENSMUST00000128647 | Chr11:62605765–62607748 | antisense | −3·5855 | 0·0065 | down | 3·0050 | 0·0246 | up |
| XR_839·1 | XR_866839·1 | Chr2:148023805–148040560 | intergenic | −1·0953 | 0·0024 | down | 1·3578 | 0·00017 | up |
| EN_301 | ENSMUST00000232301 | Chr4:132308675–132311024 | intergenic | −7·0723 | 0·0008 | down | 6·1139 | 0·0039 | up |
| EN_215 | ENSMUST00000176215 | Chr17:24528266–24528743 | antisense | −2·4040 | 0·0177 | down | 2·2243 | 0·0298 | up |
| NO_670·2 | NONMMUT037670·2 | Chr2:67565702–68073574 | sense_exon_overlap | −4·1723 | 0·0120 | down | 3·9807 | 0·0172 | up |
| EN_264 | ENSMUST00000182264 | Chr8:121059118–121083110 | antisense | −4·3240 | 0·0210 | down | 4·2427 | 0·0236 | up |
| EN_098 | ENSMUST00000181098 | Chr8:109249865–109273811 | intergenic | −1·8258 | 0·0093 | down | 3·1646 | ≤ 0·0001 | up |
| NO_699·1 | NONMMUT122699·1 | Chr6:92940238–93273001 | antisense | −3·0831 | 0·0033 | down | 3·0330 | 0·0039 | up |
| XR_008·2 | XR_870008·2 | Chr7:132874613–132897571 | sense_exon_overlap | −4·7204 | 0·0028 | down | 5·1332 | 0·0011 | up |
| *NO_902·1* | *NONMMUT148902·1* | *Chr5:28032094–28060425* | *intergenic* | *−719·4631* | *≤ 0·0001* | *down* | *21·2409* | *≤ 0·0001* | *up* |
| EN_844 | ENSMUST00000186844 | Chr10:111506574–111507662 | antisense | −3·1862 | 0·0364 | down | 4·1754 | 0·0052 | up |
| EN_995 | ENSMUST00000225995 | Chr8:57304263–57315834 | intergenic | −1·7129 | 0·0232 | down | 1·8990 | 0·0117 | up |
| EN_354 | ENSMUST00000188354 | Chr9:74852908–74855385 | intergenic | −1·2816 | 0·0293 | down | 1·9280 | 0·0010 | up |
| NO_112·1 | NONMMUT135112·1 | Chr9:91340165–91341113 | intergenic | −1·5498 | 0·0466 | down | 1·8749 | 0·0153 | up |
| NO_906·1 | NONMMUT150906·1 | Chr7:35129296–35144129 | intergenic | −5·1804 | 0·0227 | down | 6·6740 | 0·0032 | up |
| *XR_907·1* | *XR_869907·1* | *Chr7:119626518–119642645* | *antisense* | *-7·9295* | *≤ 0·0001* | *down* | *9·0159* | *≤ 0·0001* | *up* |
| EN_043 | ENSMUST00000209043 | Chr7:6 156 515–6 157 618 | bidirection | −2·4244 | 0·0489 | down | 3·2453 | 0·0074 | up |
| NR_521·1 | NR_045521·1 | Chr7:44976754–44986420 | sense_exon_overlap | −6·8159 | ≤ 0·0001 | down | 5·7477 | 0·0001 | up |
| NO_506·1 | NONMMUT152506·1 | Chr8:10869828–10892071 | intergenic | −6·0256 | 0·0125 | down | 5·8387 | 0·0156 | up |
| *NO_720·1* | *NONMMUT141720·1* | *Chr12:7 869 994–7 950 258* | *intergenic* | *-7·3934* | *≤ 0·0001* | *down* | *8·1098* | *≤ 0·0001* | *up* |
| NO_606·1 | NONMMUT080606·1 | Chr10:86658515–86671018 | intergenic | −3·7637 | 0·0169 | down | 3·2188 | 0·0438 | up |
| NO_374·1 | NONMMUT142374·1 | Chr13:52180234–52191792 | intergenic | −8·4129 | ≤ 0·0001 | down | 4·3601 | 0·0359 | up |
| NO_861·1 | NONMMUT089861·1 | Chr13:52180234–52181773 | intergenic | −1·3475 | 0·0179 | down | 1·8520 | 0·0011 | up |
| XR_698·1 | XR_001781698·1 | Chr15:55923396–55960906 | intergenic | −19·7123 | ≤ 0·0001 | down | 19·0393 | ≤ 0·0001 | up |
| XR_243·1 | XR_877243·1 | Chr18:25835803–26218752 | intergenic | −3·6345 | 0·0331 | down | 3·8252 | 0·0246 | up |
| EN_801 | ENSMUST00000164801 | Chr14:51884937–51888924 | sense_exon_overlap | 5·2439 | 0·0309 | up | −5·1527 | 0·0340 | down |
| EN_210 | ENSMUST00000203210 | Chr6:124320486–124330519 | sense_exon_overlap | 1·0342 | 0·0036 | up | −1·0039 | 0·0047 | down |
| EN_600 | ENSMUST00000146600 | Chr2:158306611–158318613 | sense_exon_overlap | 1·3115 | ≤ 0·0001 | up | −1·1356 | ≤ 0·0001 | down |
| XR_707·2 | XR_871707·2 | Chr10:79736116–79746589 | sense_exon_overlap | 7·3682 | 0·0351 | up | −7·2771 | 0·0374 | down |
| EN_792 | ENSMUST00000146792 | Chr13:85215814–85218351 | sense_exon_overlap | 6·0538 | 0·0410 | up | −5·9626 | 0·0442 | down |
| EN_676 | ENSMUST00000161676 | Chr16:30066096–30067123 | sense_exon_overlap | 5·2913 | 0·0073 | up | −5·2001 | 0·0084 | down |
| EN_506 | ENSMUST00000168506 | Chr16:32673194–32679064 | sense_exon_overlap | 1·3301 | 0·0360 | up | −1·5880 | 0·0155 | down |
| XR_222·2 | XR_867222·2 | Chr3:65945911–65958394 | sense_exon_overlap | 6·9575 | 0·0051 | up | −6·8664 | 0·0057 | down |
| EN_393 | ENSMUST00000123393 | Chr5:86071749–86097699 | sense_exon_overlap | 2·1650 | 0·0013 | up | −1·9415 | 0·0035 | down |
| NO_923·1 | NONMMUT120923·1 | Chr5:104044618–104047397 | antisense | 2·4866 | 0·0104 | up | −5·4584 | ≤ 0·0001 | down |
| EN_404 | ENSMUST00000202404 | Chr5:92326622–92328078 | sense_exon_overlap | 1·5554 | 0·0060 | up | −1·1966 | 0·0321 | down |
| NO_074·2 | NONMMUT047074·2 | Chr4:44931161–44932207 | sense_intron_overlap | 2·1056 | 0·0465 | up | −3·6282 | 0·0012 | down |
| EN_219 | ENSMUST00000139219 | Chr3:36946220–36948149 | sense_exon_overlap | 4·8551 | 0·0387 | up | −4·7639 | 0·0425 | down |
| NO_801·2 | NONMMUT009801·2 | Chr11:54697021–54698285 | sense_intron_overlap | 6·8862 | ≤ 0·0001 | up | −3·2856 | 0·0042 | down |
| XR_135·2 | XR_875135·2 | Chr15:35864333–35886870 | antisense | 1·6843 | 0·0007 | up | −1·8100 | 0·0003 | down |
| NO_835·2 | NONMMUT003835·2 | Chr11:172371731–172374084 | sense_intron_overlap | 1·4765 | 0·0290 | up | −1·6391 | 0·0167 | down |
| EN_119 | ENSMUST00000219119 | Chr10:28737424–28740885 | sense_exon_overlap | 3·7209 | 0·0042 | up | −2·8517 | 0·0221 | down |
| EN_554 | ENSMUST00000133554 | Chr16:35541144–35648140 | sense_exon_overlap | 3·3014 | 0·0013 | up | −3·5710 | 0·0010 | down |
| EN_155 | ENSMUST00000125155 | Chr7:28834155–28835853 | sense_exon_overlap | 1·2640 | 0·0115 | up | −1·2009 | 0·0166 | down |
| EN_766 | ENSMUST00000211766 | Chr7:46751870–46754313 | sense_intron_overlap | 4·5932 | 0·0004 | up | −3·3693 | 0·0045 | down |
| XR_036·3 | XR_384036·3 | Chr15:83100191–83108344 | sense_exon_overlap | 6·8851 | ≤ 0·0001 | up | −6·7940 | ≤ 0·0001 | down |
| EN_426 | ENSMUST00000182426 | Chr5:14514992–14860184 | sense_exon_overlap | 1·3282 | 0·0233 | up | −1·8959 | 0·0013 | down |
| EN_406 | ENSMUST00000141406 | Chr11:120347086–120348469 | sense_exon_overlap | 1·4937 | 0·0056 | up | −1·1063 | 0·0391 | down |
| EN_591 | ENSMUST00000222591 | Chr12:84012863–84017674 | sense_exon_overlap | 1·8649 | 0·0013 | up | −1·4006 | 0·0154 | down |
| EN_547 | ENSMUST00000210547 | Chr7:46740496–46742942 | sense_exon_overlap | 3·0360 | ≤ 0·0001 | up | −2·6489 | 0·0006 | down |

**Table 2.** (*Continued*)

| lncRNA | Full name | Genomic location | Characteristic | HFD/NFD | | | HFD + NAC/HFD | | |
|---|---|---|---|---|---|---|---|---|---|
| | | | | $Log_2FC$ | *P* | Regulation | $Log_2FC$ | *P* | Regulation |
| EN_994 | ENSMUST00000172994 | Chr17:35320404–35325099 | sense_exon_overlap | 1·7550 | 0·0009 | up | −1·0840 | 0·0341 | down |
| NO_609·1 | NONMMUT148609·1 | Chr4:109402286–109406957 | antisense | 6·8566 | ≤ 0·0001 | up | −2·5216 | 0·0447 | down |
| EN_221 | ENSMUST00000133221 | Chr17:29057429–29079179 | intergenic | 3·0885 | 0·0356 | up | −3·7239 | 0·0120 | down |
| NO_069·1 | NONMMUT147069·1 | Chr2:147944001–148040265 | intergenic | 1·9637 | 0·0033 | up | −1·8593 | 0·0054 | down |
| EN_401 | ENSMUST00000156401 | Chr4:127531621–127532885 | intergenic | 2·5031 | 0·0012 | up | −1·5985 | 0·0255 | down |
| NO_210·1 | NONMMUT148210·1 | Chr4:127522415–127533007 | intergenic | 6·3289 | ≤ 0·0001 | up | −2·7507 | 0·0347 | down |
| EN_638 | ENSMUST00000225638 | Chr13:120040092–120052178 | sense_exon_overlap | 2·2232 | 0·0399 | up | −2·1852 | 0·0442 | down |
| NO_416·2 | NONMMUT004416·2 | Chr1:192138814–192151026 | bidirection | 4·7668 | 0·0347 | up | −6·5949 | 0·0045 | down |
| NO_899·1 | NONMMUT148899·1 | Chr5:28032089–28060425 | intergenic | 1·2064 | 0·0080 | up | −1·3871 | 0·0023 | down |
| NO_981·1 | NONMMUT138981·1 | Chr1:31034546–31096654 | sense_exon_overlap | 8·2523 | 0·0249 | up | −8·1612 | 0·0265 | down |
| EN_683 | ENSMUST00000195683 | Chr12:115262683–115287908 | intergenic | 1·8017 | 0·0003 | up | −1·6300 | 0·0011 | down |
| EN_648 | ENSMUST00000201648 | Chr5:150562310–150566358 | sense_exon_overlap | 1·3666 | 0·0033 | up | −1·6057 | 0·0009 | down |
| EN_957 | ENSMUST00000204957 | Chr6:113797806–113799684 | sense_exon_overlap | 2·0553 | 0·0466 | up | −4·4311 | 0·0012 | down |
| NO_734·2 | NONMMUT060734·2 | Chr7:35128475–35144129 | intergenic | 2·1310 | ≤ 0·0001 | up | −1·2025 | 0·0090 | down |
| EN_090 | ENSMUST00000209090 | Chr7:98904267–98907902 | antisense | 3·3423 | 0·0006 | up | −2·2976 | 0·0082 | down |
| EN_859 | ENSMUST00000213859 | Chr9:44670452–44672238 | bidirection | 1·7447 | 0·0002 | up | −1·8512 | ≤ 0·0001 | down |
| NO_103·2 | NONMMUT070103·2 | Chr9:77706282–77707882 | intergenic | 2·6606 | 0·0002 | up | −1·2718 | 0·0417 | down |
| EN_199 | ENSMUST00000214199 | Chr10:93084205–93093727 | intergenic | 3·3109 | 0·0003 | up | −1·8481 | 0·0302 | down |
| NO_431·1 | NONMMUT139431·1 | Chr10:43742808–43767410 | intergenic | 2·4173 | 0·0137 | up | −2·1029 | 0·0293 | down |
| XR_040·2 | XR_872040·2 | Chr10:111599725–111611544 | intergenic | 4·6545 | 0·0016 | up | −8·8786 | ≤ 0·0001 | down |
| NO_712·1 | NONMMUT139712·1 | Chr10:99459562–99469462 | intergenic | 1·5428 | 0·0297 | up | −1·6813 | 0·0186 | down |
| EN_381 | ENSMUST00000218381 | Chr10:71168736–71182040 | intergenic | 3·8694 | 0·0017 | up | −3·0588 | 0·0098 | down |
| NO_100·2 | NONMMUT034100·2 | Chr19:20409088–20422121 | intergenic | 2·7598 | 0·0369 | up | −6·4896 | ≤ 0·0001 | down |
| NO_957·1 | NONMMUT105957·1 | Chr19:20527381–20555795 | antisense | 1·5016 | 0·0280 | up | −1·8332 | 0·0085 | down |
| NO_384·1 | NONMMUT143384·1 | Chr14:34604220–34606879 | intergenic | 1·6662 | 0·0065 | up | −2·5010 | 0·0001 | down |
| EN_074 | ENSMUST00000236074 | Chr18:84625744–84640906 | antisense | 1·9530 | 0·0035 | up | −2·1771 | 0·0017 | down |
| EN_350 | ENSMUST00000235350 | Chr17:31907878–31909029 | intergenic | 1·2976 | 0·0395 | up | −1·5989 | 0·0122 | down |

NFD, Normal fat diet; HFD, High-fat diet; NAC, N-acetylcysteine; lncRNA, long non-coding RNA.

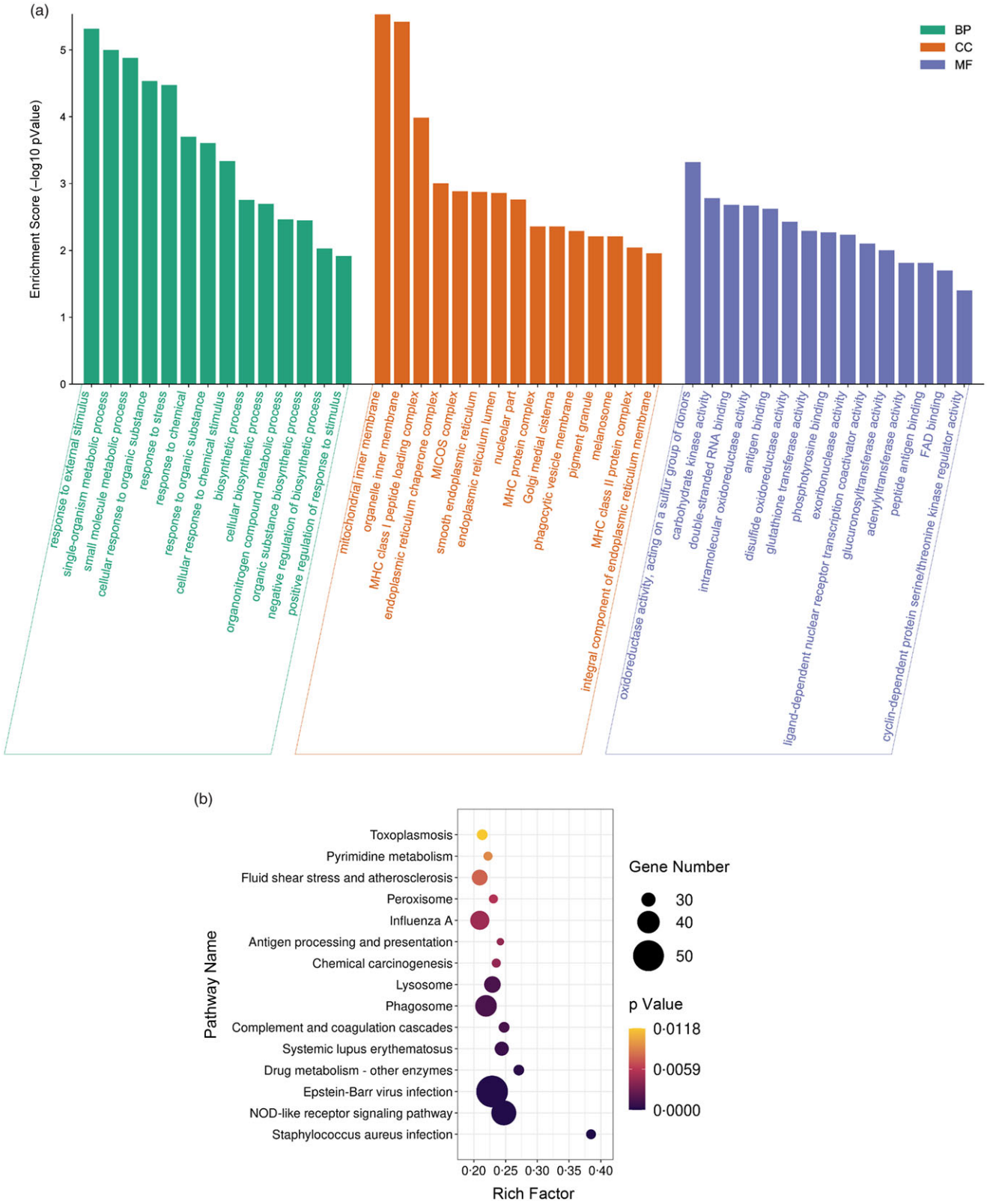


**Fig. 3.** Gene Ontology (GO) and KEGG analyses. (a) GO analysis of host genes. BP, biological process; CC, cellular component; MF, molecular function. (b) Kyoto Encyclopaedia of Genes and Genomes (KEGG) analysis of host genes. The rich factor is the ratio of the number of enriched genes in the pathway entry to the total number of genes in the pathway entry.

British Journal of Nutrition

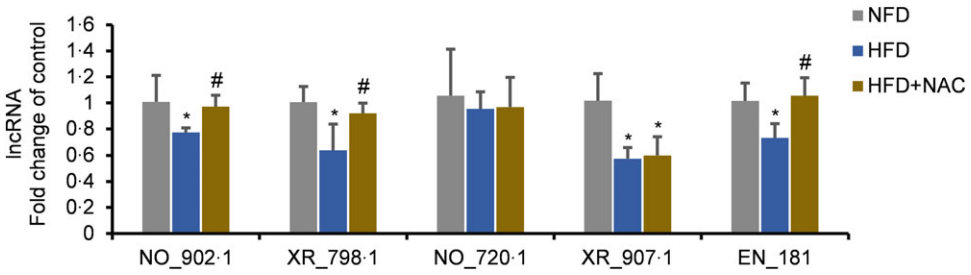


**Fig. 4.** Validation of candidate lncRNA by qRT-PCR. RNA was extracted from liver samples as described in the Methods section. qRT-PCR was performed to validate the expression of the tested lncRNA. $^{*}P < 0{\cdot}05$ *v.* the NFD group; $^{\#}P < 0{\cdot}05$ *v.* the HFD group. *n* 4 mice per group.

**Table 3.** Sequencing data of 13 mRNAs in high-fat diet HFD/NFD and HFD + NAC/HFD

| | | HFD/NFD | | | HFD + NAC/HFD | | |
|---|---|---|---|---|---|---|---|
| mRNA ID | Gene name | Regulation | $Log_2FC$ | *P* | Regulation | $Log_2FC$ | *P* |
| ENSMUST00000207394 | St5 | down | −3·4680 | 0·0225 | up | 3·7136 | 0·0142 |
| ENSMUST00000202556 | Slc5a6 | down | −3·0470 | 0·0152 | up | 4·1861 | 0·0008 |
| ENSMUST00000118812 | Fzr1 | down | −5·4603 | 0·0209 | up | 5·0806 | 0·0320 |
| ENSMUST00000049206 | Arhgef3 | down | −19·9126 | ≤ 0·0001 | up | 20·9590 | ≤ 0·0001 |
| ENSMUST00000141954 | Cd81 | down | −7·0039 | 0·0221 | up | 9·3012 | 0·0024 |
| ENSMUST00000106451 | Unc13d | down | −5·8741 | 0·0382 | up | 6·0319 | 0·0333 |
| ENSMUST00000092723 | Arid1b | down | −7·2024 | 0·0016 | up | 7·1184 | 0·0019 |
| ENSMUST00000001122 | Slc13a2 | down | −5·2025 | ≤ 0·0001 | up | 2·9164 | 0·0243 |
| ENSMUST00000066127 | Dgcr2 | down | −5·4688 | 0·0101 | up | 8·7404 | ≤ 0·0001 |
| ENSMUST00000231848 | Ahsg | down | −5·5052 | 0·0199 | up | 5·9816 | 0·0113 |
| ENSMUST00000151535 | Abcb8 | down | −2·6710 | 0·0056 | up | 2·0282 | 0·0368 |
| ENSMUST00000192985 | Zfp639 | down | −5·1369 | ≤ 0·0001 | up | 5·3864 | ≤ 0·0001 |
| ENSMUST00000162309 | Pard3 | down | −7·5281 | ≤ 0·0001 | up | 8·3667 | ≤ 0·0001 |

NFD, normal fat diet; HFD, high-fat diet; NAC, N-acetylcysteine.

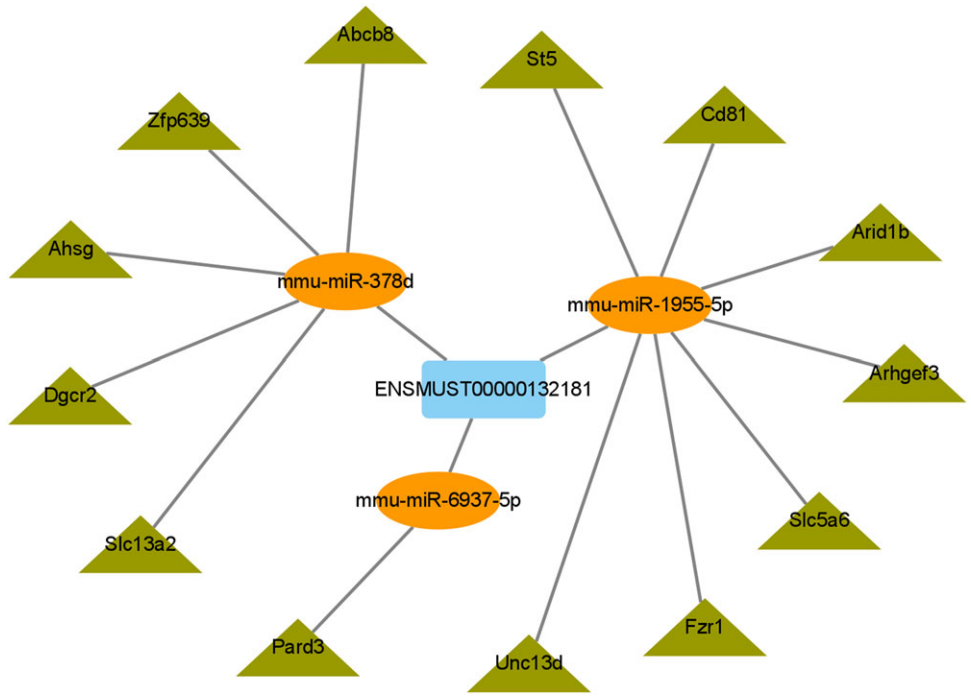


**Fig. 5.** lncRNA-EN_181-associated ceRNA network construction. The ceRNA network was constructed as described in the Methods section using Cytoscape software. The green rectangles represent mRNA, and the orange rectangles represent miRNA.

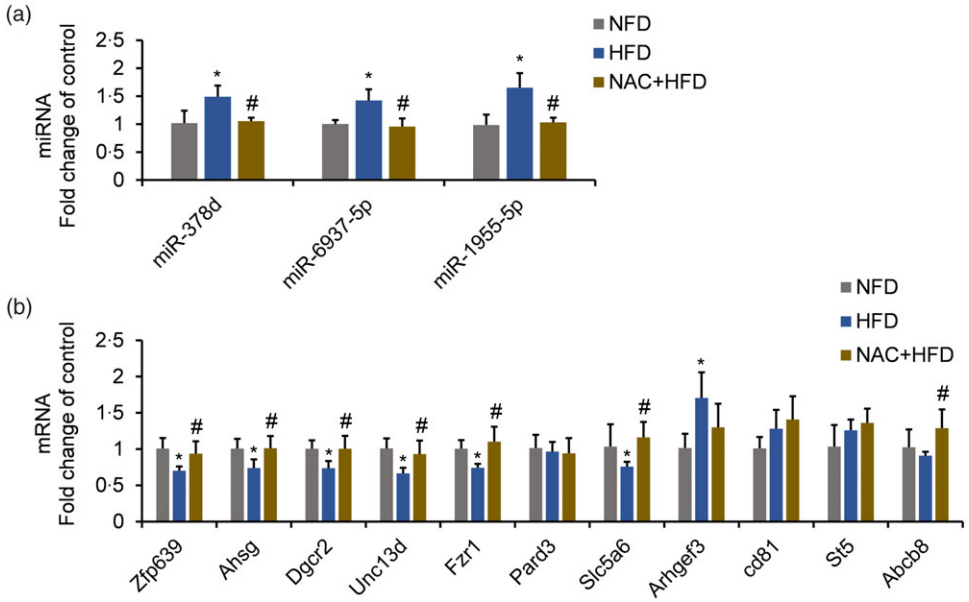


**Fig. 6.** The expressions of microRNA and mRNA corresponding to lncRNA-EN_181 by qRT-PCR. qRT-PCR was performed to validate the expression of (a) microRNA and (b) mRNA. $^{*}P < 0{\cdot}05$ *v.* the NFD group; $^{\#}P < 0{\cdot}05$ *v.* the HFD group. *n* 4 mice per group.

sequencing. Based on a FC > 2 or ≤ 0·5 and a *P* value ≤ 0·05, we explored known lncRNA expression profiles in NFD-, HFD- and HFD + NAC-treated mice livers and screened out 175 lncRNA, which were significantly up/down-regulated by HFD but were markedly reversed by NAC treatment. Subsequently, we performed GO and KEGG analysis on these 175 known lncRNA and found that the most enriched term in molecular function aspect of GO analysis was oxidoreductase active. Oxidoreductases catalyse redox reaction which is the most basic chemical reaction in human body[41]. Oxidative stress commonly occurs following redox balance disturbance, which is a well-known pathological mechanism in NAFLD[9]. As the precursor of glutathione, NAC is an important substance to reduce oxidative damage[42]. Meanwhile, the KEGG analysis revealed that peroxisome and NOD-like receptor signal pathway were the meaningful enriched pathways in our study. Peroxisomes[43] are key metabolic organelles that contribute to cellular lipid metabolism and cellular redox balance. Peroxisomal dysfunction has been linked to various metabolic disorders in humans, including NAFLD[44]. The NOD-like receptor signalling pathway has been considered a crucial regulator of inflammation-associated diseases in mammals[45,46]. Patients with severe NAFLD were found to exhibit significant up-regulation of NOD-like receptor protein 3 inflammasome components[47]. Additionally, NOD-like receptor protein 3 inflammasome functional deficiency protected mice from choline-deficient amino acid-defined diet-induced steatohepatitis[48]. Oxidative stress and inflammation have been well documented as critical mechanisms that lead to hepatic cell death and tissue injury[49]. Our findings in this study implied that these candidate lncRNA contribute to the NAC-mediated amelioration of NAFLD through oxidative stress and inflammation pathways.

For further screening, we established more stringent selection criteria, that is, $\log_2$ (FC) ≥ 4, *P* value ≤ 0·01 and *P*-adjust ≤ 0·01, and obtained five lncRNA from those 175 known lncRNA. Then, qRT-PCR was employed to verify the expression of these five lncRNA. We observed that the expression of lncRNA-NO_902·1, lncRNA-XR_798·1 and lncRNA-EN_181 was dramatically decreased by HFD feeding but increased by NAC treatment. This result was consistent with the RNA sequencing results. The ceRNA networks were subsequently constructed for those three lncRNA by taking the intersection of the miRanda and RNAhybrid database predictions. Unexpectedly, no miRNA were predicted by either the miRanda or RNAhybrid databases for lncRNA-NO_902·1 and lncRNA-XR_798·1. Only the lncRNA-EN_181-associated ceRNA network was successfully constructed in this study. Notably, we confirmed that lncRNA-EN_181, a known sense_exon_overlap lncRNA, could be successfully paired in sequences from humans by homologous sequence alignment (online Supplementary Table 2).

To the best of our knowledge, only a few studies have addressed the biofunctions of lncRNA-EN_181 in NAFLD. Our study suggested for the first time that lncRNA-EN_181 might be a potential target in HFD-induced NAFLD and provided insight into the protective role of NAC. Although how lncRNA-EN_181 regulates NAFLD is largely unclear, interpretation of the lncRNA-EN_181-associated ceRNA network might help us to determine the partners through which lncRNA-EN_181 contributes to the protective effects of NAC. Thirteen mRNA whose expression was decreased by HFD feeding but restored by NAC treatment were predicted as potential targets of lncRNA-EN_181 in a miRNA-mediated manner. In line with the results of GO and KEGG analyses, eight mRNA were associated with oxidative stress and inflammatory response pathways in various tissues. Some of them exhibit strong antioxidant effects; for example, Abcb8 is a mitochondrial inner membrane protein, and its deletion leads to mitochondrial iron overload in mouse cardiomyocytes, intracellular ROS elevation and cell death[50].

Transcriptional up-regulation of Ahsg by ProBeptigen (an extract from hydrolysed chicken) exerts preventive effects against oxidative stress in the brains of accelerated senescence-prone mice[51]. However, some of the mRNA show pro-oxidative effects; for instance, knockdown of Arid1b suppresses oxidative stress and blunts senescence in C57BL/6 mice with hepatocellular carcinoma[52]. We speculated that the HFD-mediated reduction in Arid1b expression is due to a negative feedback protection mechanism. Moreover, some mRNA have been reported to be closely associated with inflammation in various diseases and might play an anti-inflammatory role in a direct or feedback-dependent manner. Mice with embryonic intestinal-specific depletion of Slc5a6, a sodium-dependent multivitamin transporter, develop severe spontaneous intestinal inflammation[53]. The Unc13d mutation is positively associated with the development of haemophagocytic lymphohistiocytosis, an inflammation-mediated disease[54]. Pard3 has been shown to be positively associated with ulcerative colitis in humans, based on a cohort study[55]. CD81, a ubiquitously expressed membrane protein, is involved in a variety of biological responses, mostly studied in the context of the immune system[56] and lung inflammation[57]. Arhgef3 expression is positively related to excess inflammatory microglial activation in mice with spinal cord injury[58]. Additionally, the connection between the remaining five mRNA – St5, Fzr1, Slc13a2, Dgcr2 and Zfp639 – and oxidative stress and inflammatory reactions are largely unknown. In our study, verified by qRT-PCR, the expressions of miR-378d, miR-6937–5p and miR-1955–5p were up-regulated by HFD feeding but reversed by NAC; meanwhile, the expressions of *Zfp639*, *Ahsg*, *Dgcr2*, *Unc13d*, *Fzr1 and Slc5a6* were down-regulated by HFD feeding but rescued by NAC. Moreover, the expressions of *Pard3*, *Arhgef3*, *Cd81*, *St5* and *Abcb8* were not statistically different under HFD and NAC interventions. And, the expressions of *Arid1b* and *Slc13a2* were not detected in mouse liver. However, the exact mechanisms implicated in the effects of the predicted microRNA and mRNA in NAFLD are still unknown and need further investigation.

## Conclusion

In summary, we provided evidence that lncRNA function as a potential target in NAC-ameliorated NAFLD induced by HFD feeding in mice by suppressing oxidative stress and inflammation. Further analysis indicated for the first time that lncRNA-EN_181 contributes to the beneficial role of NAC via regulation of its ceRNA network. We proposed that lncRNA-EN_181 might be applied as a potential therapeutic target for the prevention and treatment of NAFLD.

## Supplementary material

For supplementary material accompanying this paper visit https://doi.org/10.1017/S0007114522001829

## Acknowledgements

This work was supported by the National Natural Science Foundations of China (81973041), Natural Science Foundation of Zhejiang Province (LR20H260001 and LZ21H030001), Special Support Program for High Level Talents in Zhejiang Province (ZJWR0308092), China Postdoctoral Foundation (2021M692892) and Research Project of Zhejiang Chinese Medical University (2021JKZDZC08).

The authors' responsibilities were as follows: S. L. initiated and designed the project. W. Y., R. G., A. P., Q. D., L. H., Q. S., and L. C. performed experiments and analysed data; X. D. and L. N. helped design the project and provided valuable advice. R. G. and S. L. wrote the manuscript. S. L. supervised the study.

The authors have declared no conflict of interest.

## References

1. Eslam M, Valenti L & Romeo S (2018) Genetics and epigenetics of NAFLD and NASH: clinical impact. *J Hepatol* **68**, 268–279.
2. Byrne CD & Targher G (2015) NAFLD: a multisystem disease. *J Hepatol* **62**, S47–S64.
3. Younossi Z, Anstee QM, Marietti M, *et al.* (2018) Global burden of NAFLD and NASH: trends, predictions, risk factors and prevention. *Nat Rev Gastroenterol Hepatol* **15**, 11–20.
4. Tilg H, Moschen AR & Roden M (2017) NAFLD and diabetes mellitus. *Nat Rev Gastroenterol Hepatol* **14**, 32–42.
5. Targher G, Byrne CD & Tilg H (2020) NAFLD and increased risk of cardiovascular disease: clinical associations, pathophysiological mechanisms and pharmacological implications. *Gut* **69**, 1691–1705.
6. Luo X, Li H, Ma L, *et al.* (2018) Expression of STING is increased in liver tissues from patients with NAFLD and promotes macrophage-mediated hepatic inflammation and fibrosis in mice. *Gastroenterology* **155**, 1971–1984.e4.
7. Tsuchida T, Lee YA, Fujiwara N, *et al.* (2018) A simple diet- and chemical-induced murine NASH model with rapid progression of steatohepatitis, fibrosis and liver cancer. *J Hepatol* **69**, 385–395.
8. Boland ML, Oró D, Tølbøl KS, *et al.* (2019) Towards a standard diet-induced and biopsy-confirmed mouse model of non-alcoholic steatohepatitis: impact of dietary fat source. *World J Gastroenterol* **25**, 4904–4920.
9. Rives C, Fougerat A, Ellero-Simatos S, *et al.* (2020) Oxidative stress in NAFLD: role of nutrients and food contaminants. *Biomolecules* **10**, 1702.
10. Aldini G, Altomare A, Baron G, *et al.* (2018) N-Acetylcysteine as an antioxidant and disulphide breaking agent: the reasons why. *Free Radic Res* **52**, 751–762.
11. Tsai CC, Chen YJ, Yu HR, *et al.* (2020) Long term N-acetylcysteine administration rescues liver steatosis via endoplasmic reticulum stress with unfolded protein response in mice. *Lipids Health Dis* **19**, 105.
12. Ma Y, Gao M & Liu D (2016) N-acetylcysteine protects mice from high fat diet-induced metabolic disorders. *Pharm Res* **33**, 2033–2042.
13. Thong-Ngam D, Samuhasaneeto S, Kulaputana O, *et al.* (2007) N-acetylcysteine attenuates oxidative stress and liver pathology in rats with non-alcoholic steatohepatitis. *World J Gastroenterol* **13**, 5127–5132.
14. de Oliveira CP, Stefano JT, de Siqueira ER, *et al.* (2008) Combination of N-acetylcysteine and metformin improves histological steatosis and fibrosis in patients with non-alcoholic steatohepatitis. *Hepatol Res* **38**, 159–165.
15. Wang H, Wang Y, Xia T, *et al.* (2018) Pathogenesis of abnormal hepatic lipid metabolism induced by chronic intermittent

hypoxia in rats and the therapeutic effect of N-acetylcysteine. *Med Sci Monit* **24**, 4583–4591.
16. Zheng J, Yuan X, Zhang C, *et al.* (2019) N-acetylcysteine alleviates gut dysbiosis and glucose metabolic disorder in high-fat diet-fed mice. *J Diabetes* **11**, 32–45.
17. Zhou H, Sun Y, Wang Q, *et al.* (2020) N-acetylcysteine alleviates liver injury by suppressing macrophage-mediated inflammatory response post microwave ablation. *Int Immunopharmacol* **85**, 106580.
18. Knoll M, Lodish HF & Sun L (2015) Long non-coding RNAs as regulators of the endocrine system. *Nat Rev Endocrinol* **11**, 151–160.
19. Chen Y, Huang H, Xu C, *et al.* (2017) Long non-coding RNA profiling in a non-alcoholic fatty liver disease rodent model: new insight into pathogenesis. *Int J Mol Sci* **18**, 21.
20. Hanson A, Wilhelmsen D & DiStefano JK (2018) The role of long non-coding RNAs (lncRNAs) in the development and progression of fibrosis associated with Nonalcoholic Fatty Liver Disease (NAFLD). *Noncoding RNA* **4**, 18.
21. Yan C, Chen J & Chen N (2016) Long noncoding RNA MALAT1 promotes hepatic steatosis and insulin resistance by increasing nuclear SREBP-1c protein stability. *Sci Rep* **6**, 22640.
22. Leti F, Legendre C, Still CD, *et al.* (2017) Altered expression of MALAT1 lncRNA in nonalcoholic steatohepatitis fibrosis regulates CXCL5 in hepatic stellate cells. *Transl Res* **190**, 25–39.e21.
23. Sun C, Liu X, Yi Z, *et al.* (2015) Genome-wide analysis of long noncoding RNA expression profiles in patients with non-alcoholic fatty liver disease. *IUBMB Life* **67**, 847–852.
24. Wu S, Lu W, Cheng G, *et al.* (2021) DAPK1 may be a potential biomarker for arterial aneurysm in clinical treatment and activated inflammation levels in arterial aneurysm through NLRP3 inflammasome by Beclin1. *Hum Exp Toxicol* **40**, S563–S572.
25. Toldo S, Mezzaroma E, O'Brien L, *et al.* (2014) Interleukin-18 mediates interleukin-1-induced cardiac dysfunction. *Am J Physiol Heart Circ Physiol* **306**, H1025–H1031.
26. Du Z, Ma Z, Lai S, *et al.* (2022) Atractylenolide I Ameliorates acetaminophen-induced acute liver injury via the TLR4/MAPKs/NF-κB signaling pathways. *Front Pharmacol* **13**, 797499.
27. Ding Q, Guo R, Pei L, *et al.* (2022) N-Acetylcysteine alleviates high fat diet-induced hepatic steatosis and liver injury via regulating the intestinal microecology in mice. *Food Funct* **13**, 3368–3380.
28. Dou X, Yang W, Ding Q, *et al.* (2021) Comprehensive Analysis of the expression profiles of hepatic lncRNAs in the mouse model of alcoholic liver disease. *Front Pharmacol* **12**, 709287.
29. Kong L, Zhang Y, Ye ZQ, *et al.* (2007) CPC: assess the protein-coding potential of transcripts using sequence features and support vector machine. *Nucleic Acids Res* **35**, W345–W349.
30. Sun L, Luo H, Bu D, *et al.* (2013) Utilizing sequence intrinsic composition to classify protein-coding and long non-coding transcripts. *Nucleic Acids Res* **41**, e166.
31. de Oliveira CP, Simplicio FI, de Lima VM, *et al.* (2006) Oral administration of S-nitroso-N-acetylcysteine prevents the onset of non alcoholic fatty liver disease in rats. *World J Gastroenterol* **12**, 1905–1911.
32. Khoshbaten M, Aliasgarzadeh A, Masnadi K, *et al.* (2010) N-acetylcysteine improves liver function in patients with non-alcoholic Fatty liver disease. *Hepat Mon* **10**, 12–16.
33. Ali MH, Messiha BA & Abdel-Latif HA (2016) Protective effect of ursodeoxycholic acid, resveratrol, and N-acetylcysteine on nonalcoholic fatty liver disease in rats. *Pharm Biolb* **54**, 1198–1208.
34. Baumgardner JN, Shankar K, Hennings L, *et al.* (2008) N-acetylcysteine attenuates progression of liver pathology in a rat model of nonalcoholic steatohepatitis. *J Nutr* **138**, 1872–1879.
35. Ozdil B, Kece C, Cosar A, *et al.* (2010) Potential benefits of combined N-acetylcysteine and ciprofloxacin therapy in partial biliary obstruction. *J Clin Pharmacol* **50**, 1414–1419.
36. Kumar P, Liu C, Hsu JW, *et al.* (2021) Glycine and N-acetylcysteine (GlyNAC) supplementation in older adults improves glutathione deficiency, oxidative stress, mitochondrial dysfunction, inflammation, insulin resistance, endothelial dysfunction, genotoxicity, muscle strength, and cognition: results of a pilot clinical trial. *Clin Transl Med* **11**, e372.
37. Kumar P, Liu C, Suliburk JW, *et al.* (2020) Supplementing glycine and N-acetylcysteine (GlyNAC) in aging HIV patients improves oxidative stress, mitochondrial dysfunction, inflammation, endothelial dysfunction, insulin resistance, genotoxicity, strength, and cognition: results of an open-label clinical trial. *Biomedicines* **8**, 390.
38. Diniz YS, Rocha KK, Souza GA, *et al.* (2006) Effects of N-acetylcysteine on sucrose-rich diet-induced hyperglycaemia, dyslipidemia and oxidative stress in rats. *Eur J Pharmacol* **543**, 151–157.
39. Sulaiman SA, Muhsin NIA & Jamal R (2019) Regulatory non-coding RNAs network in non-alcoholic fatty liver disease. *Front Physiol* **10**, 279.
40. Matboli M, Gadallah SH, Rashed WM, *et al.* (2021) mRNA-miRNA-lncRNA regulatory network in nonalcoholic fatty liver disease. *Int J Mol Sci* **22**, 6770.
41. Matsui R, Ferran B, Oh A, *et al.* (2020) Redox regulation via glutaredoxin-1 and protein S-glutathionylation. *Antioxid Redox Signal* **32**, 677–700.
42. Meyer AJ (2008) The integration of glutathione homeostasis and redox signaling. *J Plant Physiol* **165**, 1390–1403.
43. Islinger M, Voelkl A, Fahimi HD, *et al.* (2018) The peroxisome: an update on mysteries 2.0. *Histochem Cell Biol* **150**, 443–471.
44. Kersten S & Stienstra R (2017) The role and regulation of the peroxisome proliferator activated receptor α in human liver. *Biochimie* **136**, 75–84.
45. Platnich JM & Muruve DA (2019) NOD-like receptors and inflammasomes: a review of their canonical and non-canonical signaling pathways. *Arch Biochem Biophys* **670**, 4–14.
46. Kim YK, Shin JS & Nahm MH (2016) NOD-like receptors in infection, immunity, and diseases. *Yonsei Med J* **57**, 5–14.
47. Wree A, McGeough MD, Pena CA, *et al.* (2014) NLRP3 inflammasome activation is required for fibrosis development in NAFLD. *J Mol Med* **92**, 1069–1082.
48. Wan X, Xu C, Yu C, *et al.* (2016) Role of NLRP3 inflammasome in the progression of NAFLD to NASH. *Can J Gastroenterol Hepatol* **2016**, 6489012.
49. Farzanegi P, Dana A, Ebrahimpoor Z, *et al.* (2019) Mechanisms of beneficial effects of exercise training on Non-Alcoholic Fatty Liver Disease (NAFLD): roles of oxidative stress and inflammation. *Eur J Sport Sci* **19**, 994–1003.
50. Ichikawa Y, Bayeva M, Ghanefar M, *et al.* (2012) Disruption of ATP-binding cassette B8 in mice leads to cardiomyopathy through a decrease in mitochondrial iron export. *Proc Natl Acad Sci USA* **109**, 4152–4157.
51. Chou MY, Chen YJ, Lin LH, *et al.* (2019) Protective effects of hydrolyzed chicken extract (Probeptigen(R)/Cmi-168) on memory retention and brain oxidative stress in senescence-accelerated mice. *Nutrients* **11**, 1870.
52. Tordella L, Khan S, Hohmeyer A, *et al.* (2016) SWI/SNF regulates a transcriptional program that induces senescence to prevent liver cancer. *Genes Dev* **30**, 2187–2198.
53. Sabui S, Skupsky J, Kapadia R, *et al.* (2019) Tamoxifen-induced, intestinal-specific deletion of Slc5a6 in adult mice leads to

spontaneous inflammation: involvement of NF-kappaB, NLRP3, and gut microbiota. *Am J Physiol Gastrointest Liver Physiol* **317**, G518–G530.
54. Hazen MM, Woodward AL, Hofmann I, *et al.* (2008) Mutations of the hemophagocytic lymphohistiocytosis-associated gene UNC13D in a patient with systemic juvenile idiopathic arthritis. *Arthritis Rheum* **58**, 567–570.
55. Wapenaar MC, Monsuur AJ, van Bodegraven AA, *et al.* (2008) Associations with tight junction genes PARD3 and MAGI2 in Dutch patients point to a common barrier defect for coeliac disease and ulcerative colitis. *Gut* **57**, 463–467.
56. van Spriel AB (2011) Tetraspanins in the humoral immune response. *Biochem Soc Trans* **39**, 512–517.
57. Zhao W, Tan C, Yu X, *et al.* (2020) A 7-amino acid peptide mimic from hepatitis C Virus hypervariable region 1 inhibits mouse lung Th9 cell differentiation by blocking CD81 signaling during allergic lung inflammation. *J Immunol Res* **2020**, 4184380.
58. Liao L, Qian ZY, Li XY, *et al.* (2021) Disrupting RhoA activity by blocking Arhgef3 expression mitigates microglia-induced neuroinflammation post spinal cord contusion. *J Neuroimmunol* **359**, 577688.